Journal of
MATERIALS RESEARCH

Welcome Comments Help

Mechanical, tribological, and stress analyses of ion-beam-deposited boron-rich boron nitride films with increasing N content

K.F. Chan, C.W. Ong,[a] and C.L. Choy
Department of Applied Physics and Materials Research Center, The Hong Kong Polytechnic University, Hung Hom, Kowloon, Hong Kong, People's Republic of China

R.W.M. Kwok
Department of Chemistry, The Chinese University of Hong Kong, Shatin, Hong Kong, People's Republic of China

(Received 1 February 1999; accepted 26 July 1999)

Boron (B) films and B-rich BN_x films with different N contents (4.1–40.3 at.%.) were deposited by dual ion-beam deposition. The films consist of a B-rich phase constructed of icosahedral atomic clusters and a graphitelike boron nitride phase. The films with N content ≤20.3 at.% is dominated by the B-rich phase. Their hardness rises with increasing N content to reach a maximum value of 18.8 GPa. The hardness-to-elastic modulus ratio (H/E) and the critical load of the films also increase, showing stronger wear resistance of the films. These results can be explained if some N–B–N chains are formed at the interstitial sites in the network of the B-rich phase, which cross-link different icosahedral atomic clusters in the B-rich phase and strengthen the rigidity of the structure. For the films with higher N contents, the volume fraction of the graphitelike boron nitride phase becomes higher, and the hardness drops as a consequence. However, the change in the H/E ratio is rather mild. This implies that the wear resistance of the films is not altered and explains why the critical load of the films remains almost unchanged. In addition, the friction coefficient μ of all the films depends on the normal load L in the form of $\mu = aL^y$, where a and y are numerical parameters and are insensitive to the change in the N content. Furthermore, compressive stress was found to increase from about 0.12 to 1.7 GPa when the N content increased from 4.1 to 40.3 at.%.

I. INTRODUCTION

Boron (B)-rich solids generate a class of superhard materials constructed of a network of B-based icosahedral atomic clusters. For instance, a rhombohedral unit cell of α-rhombohedral B (α–B) comprises B icosahedral clusters at its vertices. A boron icosahedral cluster is constructed of 12 B atoms located at the vertices of an icosahedron (denoted as B_{12}).[1] Based on this framework, a number of binary B-rich solids are generated by adding a second type of atoms (e.g., C, N, or O) into boron.[2–6] For example, B_4C contains C-B-C chains located at the interstitial sites surrounded by icosahedral atomic clusters. The chains cross-link the clusters and result in a greater hardness. A similar cross-linking effect is proposed to occur in B-rich boron nitride by N–B–N chains, so that the material is also expected to be very hard.[2,3,6] However, the mechanical and tribological properties of B-rich boron nitride as functions of N content have not been systematically reported.

In this study, we investigated the correlation between the structure and the mechanical properties of ion-beam-deposited B-rich boron nitride films with different N contents. X-ray photoelectron spectroscopy (XPS), x-ray diffraction (XRD), and infrared absorption (IR) were used to examine the film composition and chemical structure, and nanoindentation and nanoscratch techniques were used to observe the hardness, elastic modulus, friction coefficient, and critical load of the films. The scanning electron microscope (SEM) images of the scratch tracks were inspected to examine the damage mechanisms of the films by scratching. The internal stress in the films was evaluated by determining the radius of curvature of the film-on-substrate configuration. The overall objective of the work is to verify whether the hardness of the B-rich boron nitride films could be enhanced with incorporation of N due to possible formation

[a] Address all correspondence to this author.

 © 1999 Materials Research Society

CAMBRIDGE JOURNALS
http://journals.cambridge.org Downloaded: 27 Aug 2013 IP address: 158.132.161.52

of some atomic chains. Furthermore, the results may reveal information about the tribological properties and internal stress of B-rich BN_x with a systematic increase in the N content, which has not been widely investigated before.

II. SAMPLE PREPARATION

The dual ion-beam system used for preparing BN_x films is described in detail elsewhere (Fig. 1),[7] which has two 3-cm Kaufman-type ion guns (Ion Tech, Inc., model 3-1500-100). Before deposition the system was pumped down to a background pressure of 2×10^{-6} torr. The substrate (100) silicon or fused quartz, was heated up to 620 °C and rotated with a speed of 2.7 rotations per minute to ensure uniformity of the films. An Ar^+ beam (1200 eV, 70 mA) was then generated by one of the ion guns to sputter a 4-inch (10.16 cm) B target. Meanwhile, an admixture of Ar and N_2 was admitted into the other ion gun to generate an assist ion beam containing Ar^+ and N_2^+ ions (160 eV, 12 mA), which bombarded the substrate for introducing N into the deposits. The total flow rate of the admixture was fixed to be 33.5 sccm by means of two mass flow controllers (MKS, model 1259). The relative fraction of N_2 (denoted as $f\ N_2$) was varied from 0 to 1 (Table I). With a fixed total flow rate, the working pressure during deposition was kept constant at 5×10^{-5} torr for all runs, so that the change in the properties of the films could mainly be ascribed to the compositional change in the films. The incident angle of the assist ion beam was adjusted at 16° from the normal of the substrate. The deposition time for all runs was fixed at 120 min.

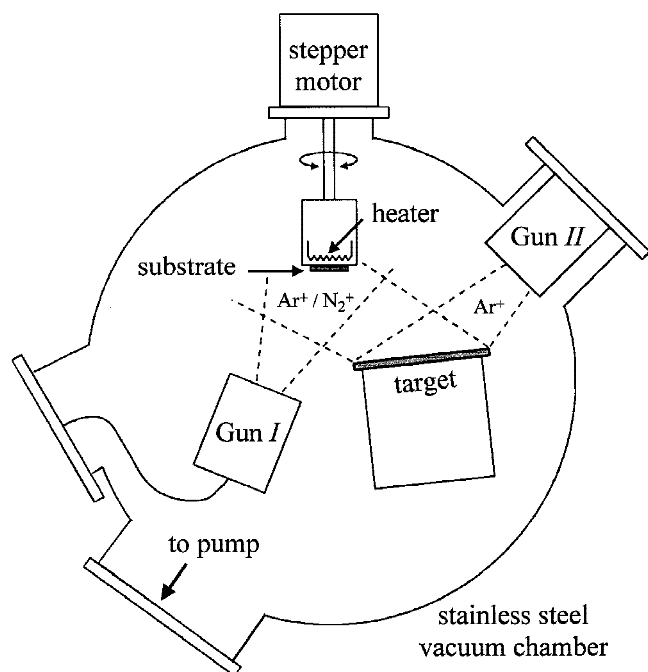

FIG. 1. Schematic diagram of the dual ion-beam system used for preparing BN_x films.

TABLE I. Fractional flow rate of N_2 admitted into the assist gun (f_{N_2}), and the N content, B content, thickness and coating rate of the B-rich BN_x films on Si.

Sample	f_{N_2}	N content (at.%)	B content (at.%)	Thickness on Si (nm)	Coating rate on Si (nm min^{-1})
1	0	2.2	92.1	304	2.53
2	0.03	4.1	89.8	317	2.64
3	0.09	9.7	84.4	341	2.84
4	0.15	11.9	83.9	380	3.17
5	0.24	20.2	75.9	402	3.35
6	0.48	28.9	66.9	496	4.13
7	0.75	38.5	57.4	566	4.72
8	1.00	40.2	56.8	620	5.17

As listed in Table I, the thickness of the films (on Si substrates) determined with an α-step surface profiler (Tencor 500) increases continuously from 304 to 620 nm. Results for the films on fused quartz are similar. Correspondingly, the coating rate rises monotonically 2.53–5.17 nm min^{-1}. This is because the Ar^+ ions in the assist beam induce more serious resputtering of the deposits than the N_2^+ ions, such that the film thickness rises when the fraction of the N_2^+ ions in the assist beam increases.

III. CHARACTERIZATION

The relative contents of B, C, N, and O in the films as functions of $f\ N_2$ were determined with a VG Scientific XPS analyzer (Al K_α 1486.7 eV). Before the measurements, the film surface was cleaned with Ar^+ ions at 4 keV and 20 mA for 5 min. The Shirley background of each spectrum was removed before counting the peak area and determining the peak position.[8]

XRD was carried out with a Philips X'PERT x-ray diffractometer (Cu K_α radiation) to inspect the crystallinity of the films. The x-ray optics for thin film geometry was used, where the incident angle of the x-ray beam fixed at a small angle of 0.75°, and the detector was controlled to scan from $2\theta = 15$ to 60°.

The information on the chemical bonds between the atoms with increasing N content was achieved by observing (i) the IR absorption spectra in the wavenumber range 400–4000 cm^{-1} using a Nicolet Magna-TR system model 750 Fourier transform IR absorption spectrometer, and (ii) the chemical shifts of the components deconvoluted from the B 1*s* photoelectron spectra.

The hardness and elastic modulus of the films as functions of N content were measured with a nanoindenter (Nano Instruments Inc., model IIs) equipped with a Berkovich diamond tip. For each maximum load, five repeti-

CAMBRIDGE JOURNALS
http://journals.cambridge.org Downloaded: 27 Aug 2013 IP address: 158.132.161.52

tive indentations were made at different points on the film surface to obtain an average result. The maximum loads of the indentations were set to vary in the range 70 μN to 80 mN. Data corresponding to indentation depths around 20 nm were assigned to represent the true mechanical properties of the film, where the error due to substrate deformation was negligible.

The nanoindenter was then operated in the scratching mode with another Berkovich diamond tip to carry out nanoscratch tests. The information on the friction coefficient and critical load of the films with different N contents were attained. In a nanoscratch test, the tip was driven to scan across the film surface by a distance of 500 μm with a speed of 5 $\mu m\ s^{-1}$. Meanwhile the normal load is applied either (i) at a constant load, or (ii) with a constant loading rate. These two methods are referred as the constant load scheme and ramping load scheme in the following discussions.

The SEM images of the scratch tracks were taken immediately after scratching in order to inspect the damage mechanism of the films. The images of the same scratch tracks were taken 2 months later to examine whether they would extend as time proceeded. The data were found to be able to reveal indirectly some information on the internal stress in the films and how the stress affected the stability of adhesion of the films on substrates.

The internal stress in the films on Si substrates was measured by determining the radius of curvature of the film-on-substrate configuration with an optical system as shown in Fig. 2.[9] A He–Ne laser (20 mW) was focused on the film with a lens of a focal length $f = 1$ m. The laser beam reflected from the film surface was then directed to shine on a position sensor. When the film was moved laterally by Δx, the laser beam shining on the sensor was shifted by ΔD. ΔD was converted from a voltage signal by a conversion factor determined through some calibration procedures. The radius of curvature of the specimen is

$$R = 2 f \Delta x / \Delta D \quad .$$

From the Stoney equation,[10] the internal stress in the film is determined as

$$\sigma_f = \frac{E_s}{(1 - \nu_s)} \cdot \frac{t_s^2}{6 \cdot R \cdot t_f} \quad , \tag{1}$$

where E_s and ν_s are Young's modulus and Poisson's ratio of the substrate, t_s and t_f the thickness of the substrate and film. $E_s/(1 - \nu_s)$ is equal to 180.5 GPa for Si,[11] and $t_s = 0.5$ mm.

IV. RESULTS AND DISCUSSIONS

A. Elemental composition

Results of XPS analyses show that after cleaning the film surface with Ar^+ ions, the measured C content drops from 30–44 at.% to 0.3–2 at.%, and the O content drops from 15–23 at.% to 1.6–4.5 at.% (Fig. 3). This indicates that the C and O atoms are located mainly at the film surface and will not affect the properties of the films significantly. As shown in Table I and Fig. 3, when fN_2 increases from 0 to 1, the N content increases monotonically from 2.2 to 40.2 at.%, whereas the B content drops from 92.1 to 56.8 at.%. This range of N-to-B ratio is appropriate for this study, as it covers the B-rich regime and approaches that of the stoichiometry of the well known hexagonal and cubic boron nitride phases.

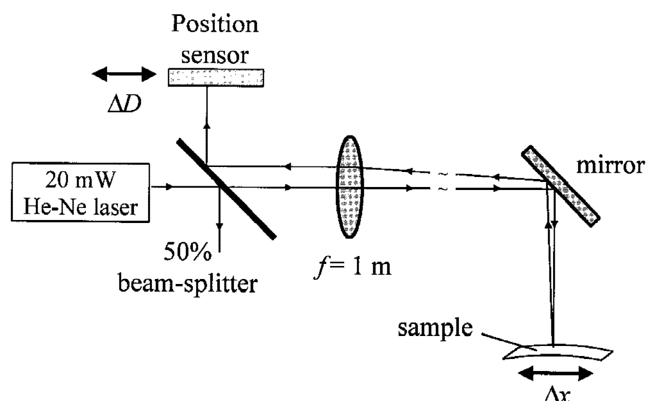

FIG. 2. Schematic diagram of the stress measurement system.

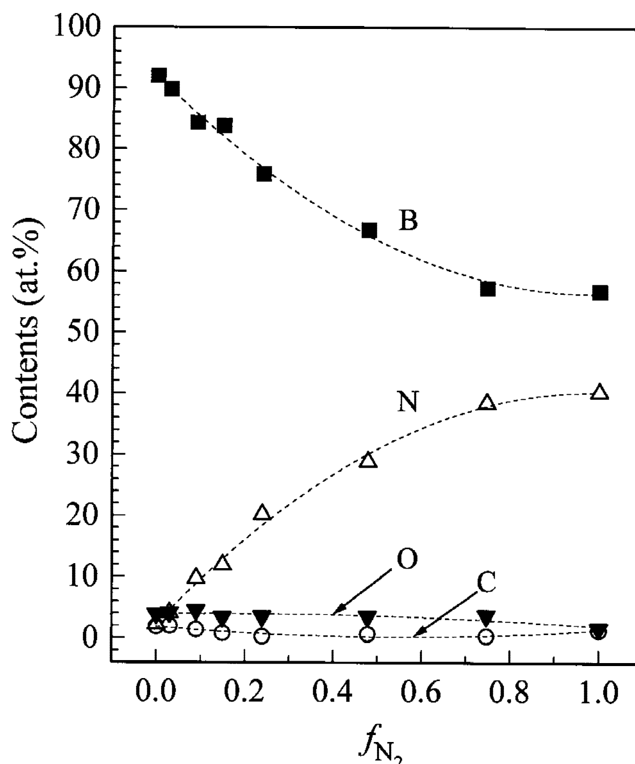

FIG. 3. Composition of BN_x films as a function of f_{N_2} after surface cleaning.

CAMBRIDGE JOURNALS
http://journals.cambridge.org Downloaded: 27 Aug 2013 IP address: 158.132.161.52

B. XRD

For the films with low N contents, a broad XRD halo centered at around 2θ = 30° is recorded as shown in Fig. 4. The halo is still clearly seen even when the N content in the films is increased to 20.2 at.%. The halo is so broad that the film is considered to be in an amorphous state. Its range roughly covers that of the two halos of amorphous boron films produced by chemical vapor deposition in the range of 2θ = 20 to 25° and 34 to 38°, respectively.[12] This leads one to infer that icosahedral atomic clusters exist in the low N-containing BN_x films up to a N content of 20.2 at.%.

We note that the range of the halo also covers the peak positions of four diffraction peaks of crystalline B-rich boron nitride films at 2θ = 23.26, 31.35, 34.73, and 37.43°.[6] Saitoh *et al*. proposed a structure for this material as depicted in Fig. 5, in which a N–B–N chain is formed inside a rhombohedral unit cell to cross-link the icosahedral atomic clusters. A stronger rigidity of the solid results. This further confirms that our low N-containing BN_x films is constructed of a network of icosahedral atomic clusters. However, because the peak positions of these diffraction peaks fall in the range of the broad halos of amorphous boron, there is no direct evidence to show the presence of interstitial N–B–N chains as conjectured by the structural model shown in Fig. 5.

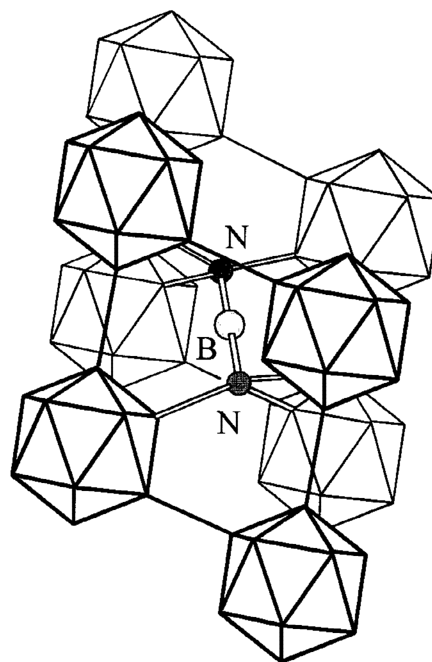

FIG. 5. Structural model of B_4N, showing the cross-linking effect by the interstitial N–B–N chains.

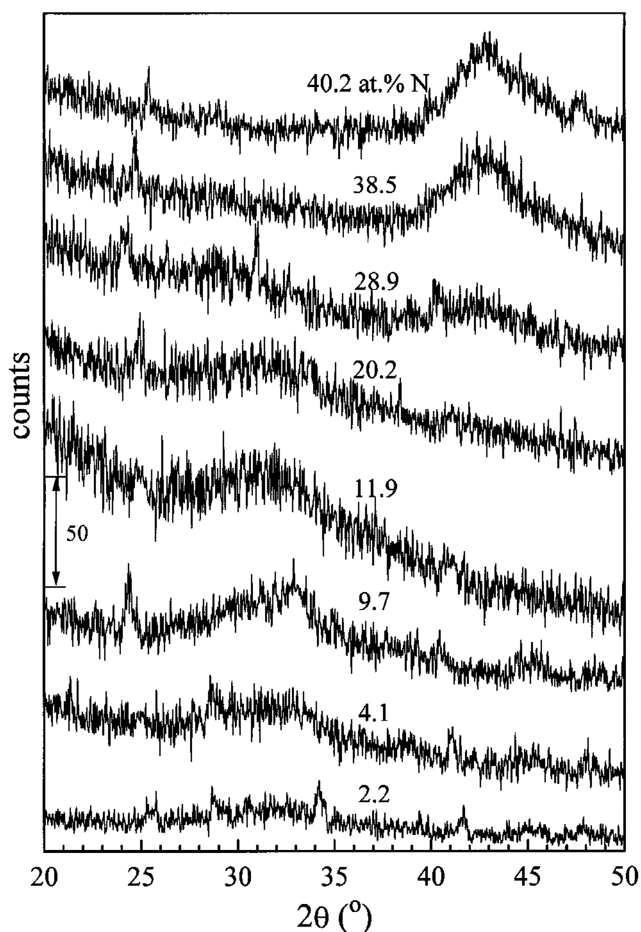

FIG. 4. XRD spectra of the BN_x films with various N contents.

For the films with N contents higher than 20.2 at.%, the above broad halo diminishes, while another broad halo centered around 42° emerges instead. According to Friedmann *et al*.,[13] this spectrum can be assigned to the (100) planes of a hexagonal boron nitride (h-BN) structure. It is thus suggested that the films with higher N contents are mainly constructed of a graphitelike boron nitride phase, which is structurally analogous to the hexagonal BN phase.

C. IR absorption

As shown in Fig. 6, the IR absorption spectra of the BN_x films with low N contents have a broad absorption band ranging from 600 to 1500 cm^{-1}. This range is basically consistent with the peak positions of some IR absorption bands of crystalline boron at 485, 550, 614, 680, 768, 848, and 925 cm^{-1}.[14] It also matches with that of the broad band of chemical vapor deposited amorphous boron films, lying from 580 to 1300 cm^{-1}.[15] This result confirms again that the low N-containing BN_x films are constructed of random networks of icosahedral atomic clusters.

When the N content continuously increases, the broad band diminishes progressively, while other two absorption bands centered at 780 and 1400 cm^{-1} appear instead. They are attributable to the out of plane B–N–B bending

CAMBRIDGE JOURNALS
http://journals.cambridge.org Downloaded: 27 Aug 2013 IP address: 158.132.161.52

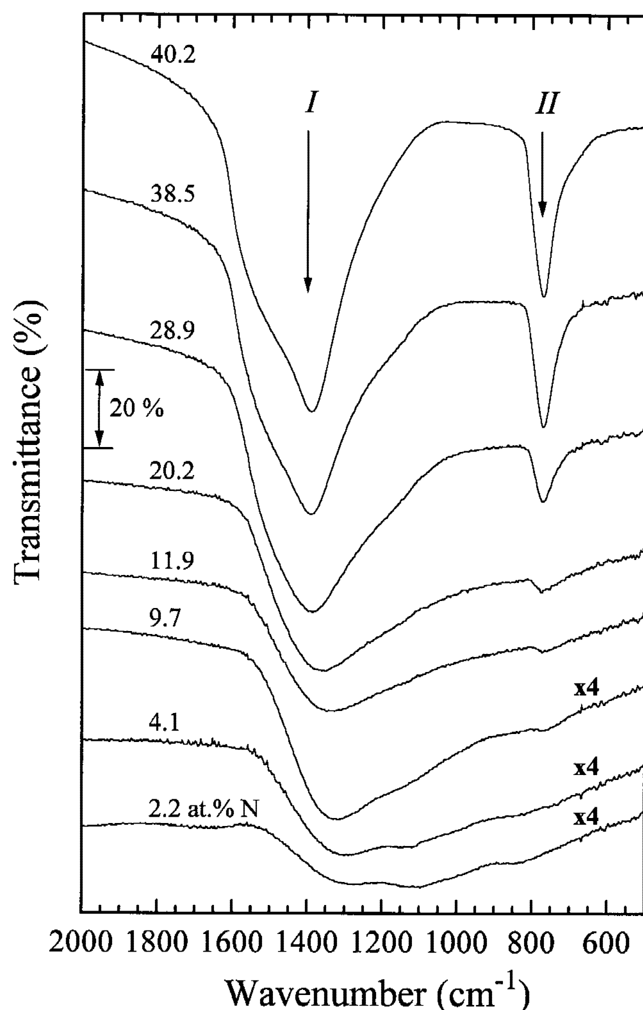

FIG. 6. IR absorption spectra of the BN_x films with various N contents.

mode and in-plane B–N stretching mode of the h-BN structure.[16,17] This indicates that the increasing incorporation of N will suppress the formation of icosahedral atomic clusters and at the same time force the graphitelike boron nitride phase to form. It appears that the band at 1400 cm^{-1} starts to be observable when the N content is low. The features of the spectra change gradually, indicating that no abrupt phase change occurs in the course of increasing N content in the films. More likely, the films are solid admixtures of a B-rich phase of icosahedrons and a phase of graphitelike boron nitride, where their relative contents are altered progressively with the increase in the N content.

D. XPS analyses

We first presume that the C 1*s* photoelectrons detected in the XPS analyses mainly come from the graphite structure in the films. The peak energy of the C 1*s* spectra mostly deviates slightly from that of graphite at 284.5 eV due to the effect of surface charging. With the C 1*s* line as a reference, the energy axis of the whole spectrum is readjusted in order to correct for such an erroneous energy shift.

Figures 7(a)–7(d) show some selected B 1*s* spectra of the films with various N contents. Each spectrum is resolved into a B^1 component and a B^2 component. Each component comprises 70% Lorentzian and 30% Gaussian constituents. The peak energy of the B^1 component is consistent with that of boron at 189.4 eV,[18] showing that the films contain some icosahedral atomic clusters. The B^2 component has the peak energy to be consistent with that of the hexagonal BN at 191.2 eV,[19,20] indicating the appearance of the graphitelike boron nitride phase in the films. With increasing N content from 4.1 to 40.2 at.%, the fraction of the B^1 component drops from 94 to 26 %, while that of the B^2 component correspondingly rises from 6% to 74%. This trend agrees with that reflected by XRD and IR absorption—that the random network of the B-rich phase constructed of icosahedral clusters is dissociated with increasing incorporation of N, whereas the graphitelike boron nitride phase grows and finally dominates the film structure. We also notice that the peak energy of the N 1*s* spectra (not shown here) shifts toward that of the hexagonal BN structure at 398.3 eV, further confirming the growth of the graphitelike boron nitride structure with the introduction of N.[21]

E. Nanoindentation

The hardness and elastic modulus of the boron films are found to be 12.8 and 193.5 GPa, respectively (Fig. 8). These values are found to be smaller than those reported by Doughty *et al*. for boron films prepared by plasma-assisted magnetron sputtering (28 and 240 GPa),[22] possibly because a much harder boron carbide phase is formed in their samples.

Figure 8 shows that the hardness and elastic modulus of the films increase with N content first and reach maximum values of 18.8 and 222 GPa at a N content of 20.3 at.%. Because the films of this group are mainly constructed of icosahedral atomic clusters, the hardening with increasing N content is explained if the B_4N structure proposed by Saitoh *et al*. is formed (Fig. 5),[6] in which N–B–N chains cross-link the icosahedral clusters to enhance the hardness of the films.

When the N content exceeds 20.3 at.%, both the hardness and elastic modulus of the films drop. This is attributed to the growth of the graphitelike boron nitride phase, which is expected to be softer. In particular, the hardness of the film with 40.2 at.% N is 13.8 GPa, which is very close to that of BN films in the hexagonal structure (13 GPa).[7]

In Fig. 9, we plot the *H*/*E* ratio against the N content. This value is expected to reflect the wear resistance of a material by scratching.[23] A higher *H*/*E* ratio means that, on the one hand the material has a higher hardness to

CAMBRIDGE JOURNALS
http://journals.cambridge.org Downloaded: 27 Aug 2013 IP address: 158.132.161.52

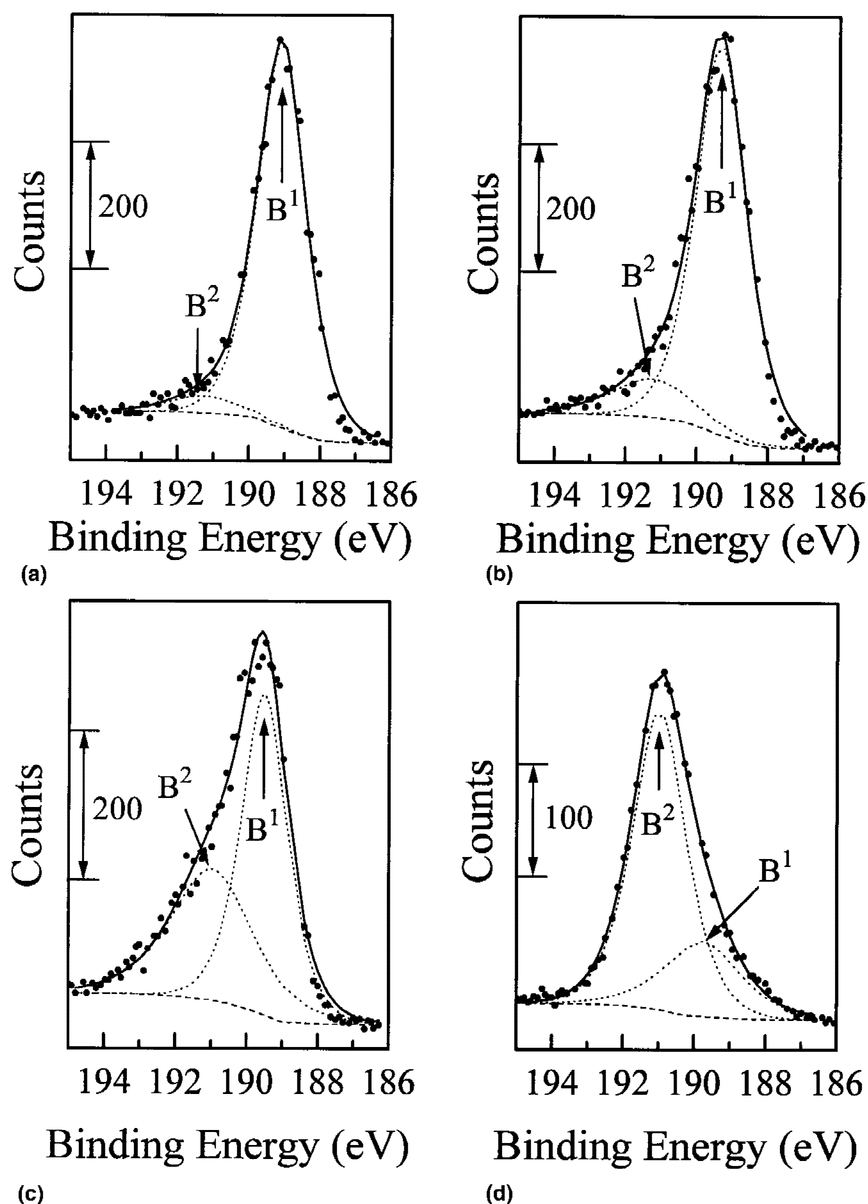

FIG. 7. B 1s spectra of the BN_x films with (a) 4.1 at.% C, (b) 9.7 at.% C, (c) 20.2 at.% C, and (d) 40.2 at.% N.

resist plastic deformation in a contact event, and on the other hand it has a small elastic modulus to give a larger elastic deformation for spreading out the normal load applied on it, so that less plastic wear is generated.

Results show that when the N content increases from 2.2 to 20.2 at.%, H/E rises prominently from 0.066 to 0.085, because the hardness rises more rapidly than the elastic modulus. For the films with higher N contents, the change in H/E is mild because both the hardness and elastic modulus drop concurrently. This trend leads to a conjecture that the wear resistance of BN_x is strengthened at first up to a N content of about 20.2 at.%, and then it is kept almost unchanged for more N incorporation. This postulation appears to be supported by the results of critical loads as presented in the next section.

F. Friction coefficient and critical load

For measuring the friction coefficient of the films, both the constant load and ramping load schemes were used. In the constant load scheme, a constant load of 0.7 or 2.5 mN was maintained during scratching. In the ramping load scheme, the load was increased with a constant rate of 0.15 mN s^{-1}, so that a maximum load of 15 mN was reached. Figure 10 shows the friction coefficients between BN_x films and diamond couple. First, the profiles of μ are smooth, indicating that, in this load range, catastrophic damage or delamination of the films does not happen, while only plastic wear can be generated. Second, associated with such situations, Miyoshi proposed that μ would depend on the normal load L in the form $\mu = aL^y$.[24] By fitting the experimental data, the

CAMBRIDGE JOURNALS
http://journals.cambridge.org Downloaded: 27 Aug 2013 IP address: 158.132.161.52

values of a and y are determined to be 0.07 and 0.4, which are insensitive to the N content of the films. Third, the results obtained by the constant load scheme, as indicated by solid dots in the figure, obey the same trend. The typical value of μ of BN_x against diamond at a normal load of 2.5 mN is about 0.1.

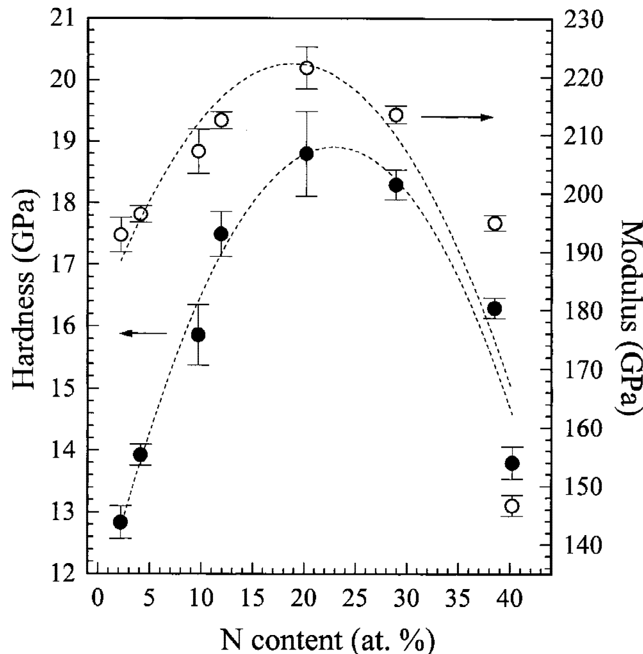

FIG. 8. Hardness and elastic modulus of the BN_x films with various N contents.

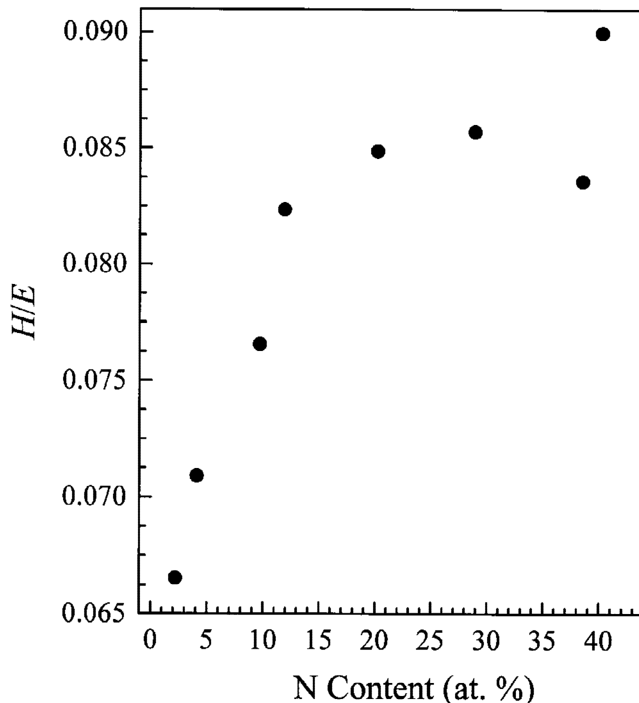

FIG. 9. H/E ratio as a function of the N content in the films.

Nanoscratch tests with a faster loading rate of 0.5 mN s^{-1} were also carried out for determining the critical load (*CL*) the films. Figure 11 shows the depth profiles of the scratch tracks made on three representative film samples containing different N contents. First, the profile recorded during scratching always lies below that recorded after scratching (postscan profile), because the former includes both the plastic and elastic deformation of film and the substrate. Second, the postscan profile starts smoothly and then becomes zigzag at some point, as denoted by *A*. The positions of points *A* are most conveniently identified by referring to the SEM images of the scratch tracks as shown in Figs. 12 (a), 13(a), and 14(a). In each picture, three scratch tracks produced repetitively with the same conditions are seen, from which the average position of *A* is determined. From these data and the loading rate of the scratching, the critical load of the films is calculated and is shown in Fig. 15. Error bars are estimated from the scattering of the position of *A*. One sees that *CL* first increases slightly with increasing N content and then remains almost flat for the films with higher N contents. It should be meaningful to correlate the data of *H*/*E* and *CL,* as the former is assigned conceptually to reflect the wear resistance of a coating, whereas the later is an experimental measure of a related property of the film. Indeed, *H*/*E* and *CL* show an almost

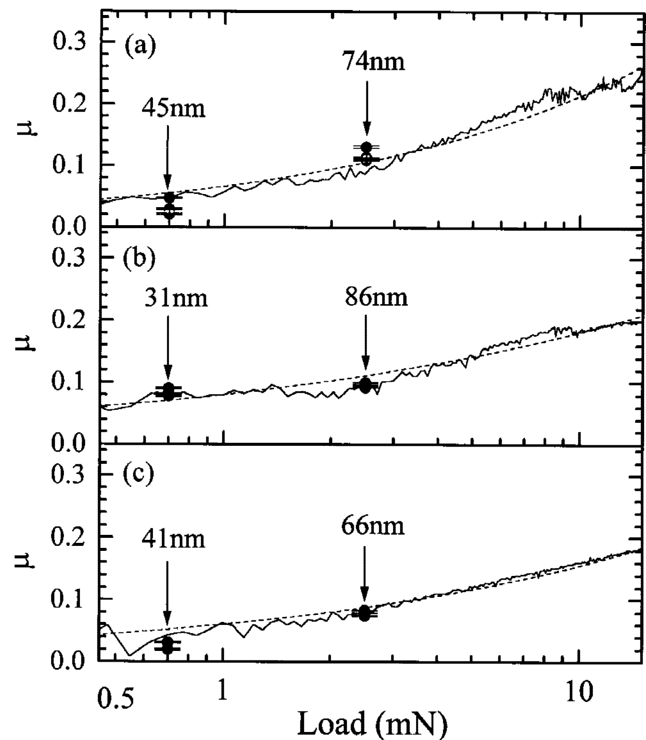

FIG. 10. Profiles of μ recorded by the ramping scheme and the constant load scheme (●). Numbers represent penetration depths of the tip for the constant load scratching. (a) 2.2 at.% N, (b) 20.2 at.% N, and (c) 40.2 at.% N.

CAMBRIDGE JOURNALS
http://journals.cambridge.org Downloaded: 27 Aug 2013 IP address: 158.132.161.52

linear correlation as indicated in Fig. 16, although scattering of the data is seen because of the difficulty in accurately locating the position of point *A* in a scratch track. We note that the data of the critical load of the films do not show a maximum value concurrent with the appearance of the maximum hardness at a N content of 20.2 at.%. Even the hardness of the films drops with a further increase in the N contents, but the critical load remains about the same. This verifies that the *H*/*E* ratio of a film is actually more effective than the hardness alone in reflecting the wear resistance of a film.

G. Damage mechanism

Figures 12(b), 13(b), and 14(b) show the SEM images of the scratch tracks on the films with increasing N contents, from which the damage mechanism by scratching can be inspected. First, the film with low N content [Fig. 12 (b)] buckles around the scratch track, and there is very little fragmentation. This indicates that the film has compressive stress and is relatively ductile. With increasing N content, the films show less buckling, but more fragments are produced. In particular, the film with the highest N content of 40.2 at.% was completely delaminated from the substrate along the path where the diamond scratched it. In addition, no buckling can be observed. This reflects that the films with higher N contents are more brittle.

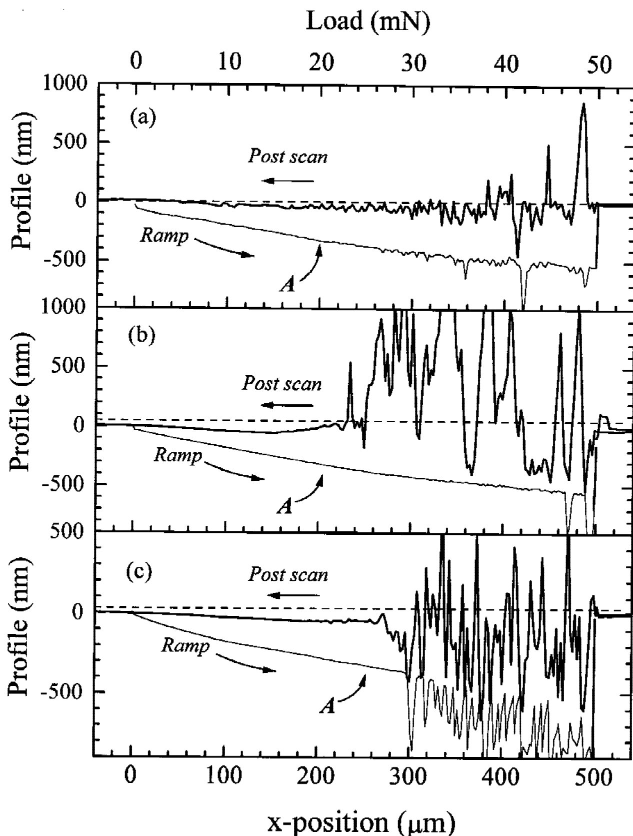

FIG. 11. Profiles of the ramping segments and postscan segments for films with (a) 2.2 at.% N, (b) 20.2 at.% N, and (c) 40.2 at.% N.

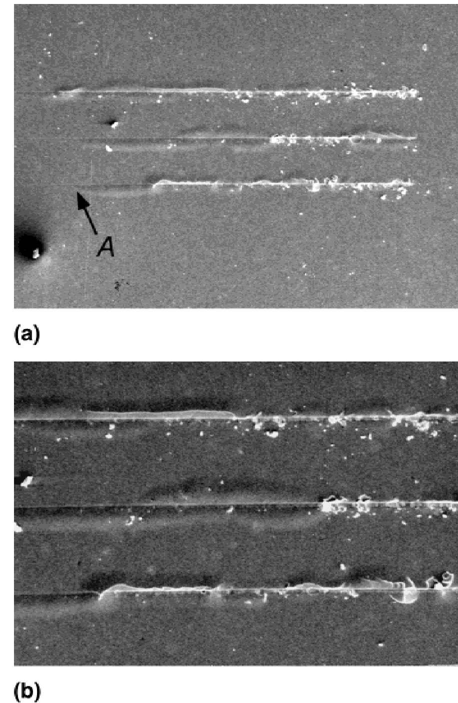

FIG. 12. SEM images of scratch tracks on the films of 2.2 at.% N just after scratching: (a) ×149, (b) ×274.

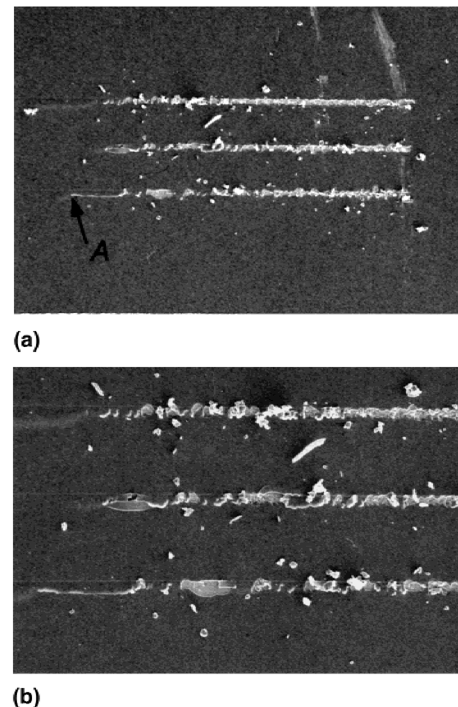

FIG. 13. SEM images of scratch tracks on the films of 20.2 at.% N just after scratching: (a) ×149, (b) ×274.

CAMBRIDGE JOURNALS
http://journals.cambridge.org Downloaded: 27 Aug 2013 IP address: 158.132.161.52

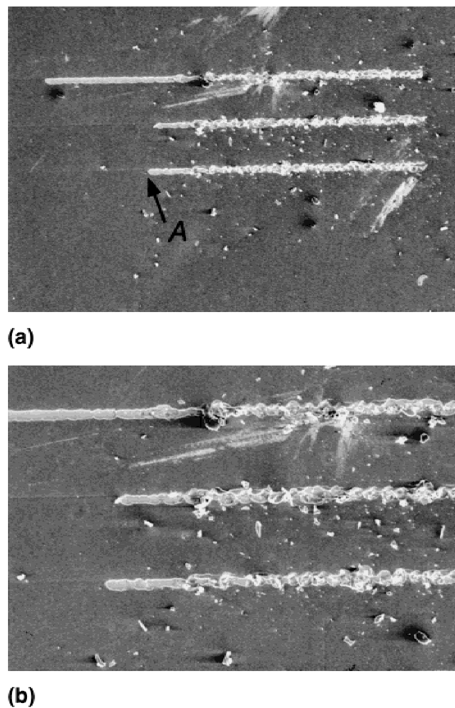

FIG. 14. SEM images of scratch tracks on the films of 40.2 at.% N just after scratching: (a) ×149, (b) ×274.

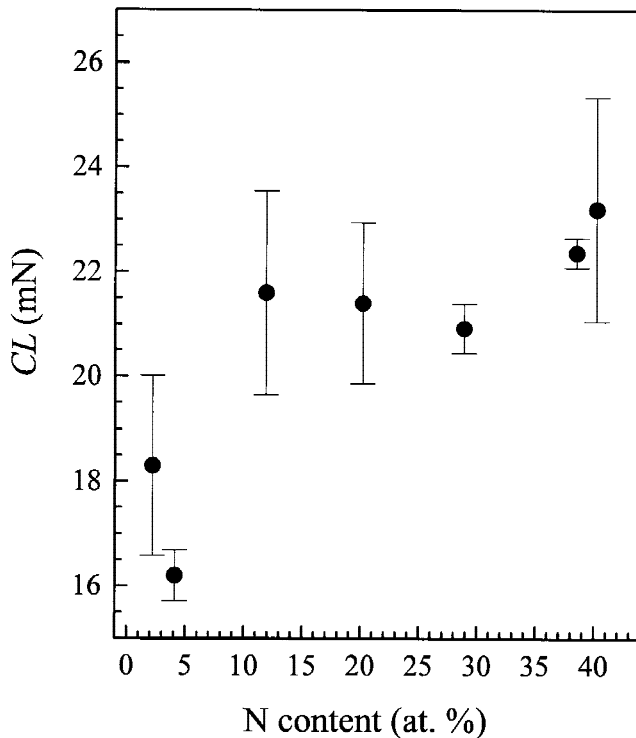

FIG. 15. Critical load of the BN_x films with various N contents.

To examine the adhesion stability of the films, we examined the SEM pictures of the same scratch tracks 2 months later as shown in Figs. 17(a) to 17(c). Comparing Figs. 17(a) to 17(c) with Figs. 14(a) to 14(c) with the same magnification, one sees that the films peel off along the scratch tracks and the delamination propagates. In particular, the film with lower N content peeled off in the form of buckling, whereas that with high N content delaminated in the form of relatively rigid fragmentation. These features further confirm that the films become more brittle when more N is added. One may further suggest that noticeable internal stress is established in the films. Figure 18 shows the results of the internal stress measurements. One can see that with increasing N content, the internal stress in the films rises prominently in a linear manner from 0.12 to 1.6 GPa. The low internal stress in the low N-containing film explains why it peels off in the form of buckling once damage is produced on the surface. On the other hand, the high internal stress in the high N-containing film is responsible for the fragmental expansion of the scratch track.

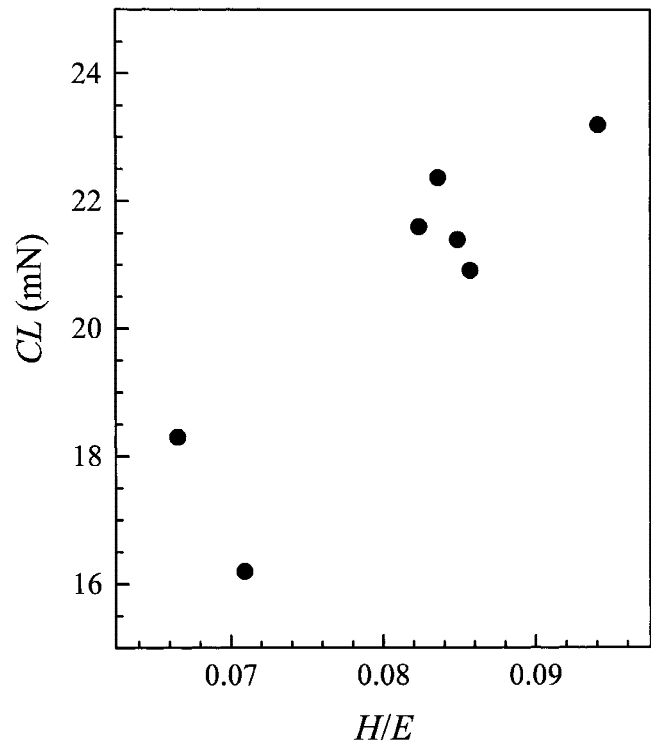

FIG. 16. Correlation between the H/E ratio and critical load of the BN_x films.

V. CONCLUSION

In conclusion, a series of boron and B-rich BN_x films with a systematic increase in N content were prepared by dual ion-beam deposition. According to IR absorption and XPS analyses, we suggest that the films are solid admixtures of a B-rich phase constructed of icosahedral atomic clusters and a graphitelike boron nitride phase. With the N content increasing from 2.2 to 20.2 at.%, the film structure is dominated by the B-rich network of icosahedral clusters, with the film hardness rising from

CAMBRIDGE JOURNALS
http://journals.cambridge.org Downloaded: 27 Aug 2013 IP address: 158.132.161.52

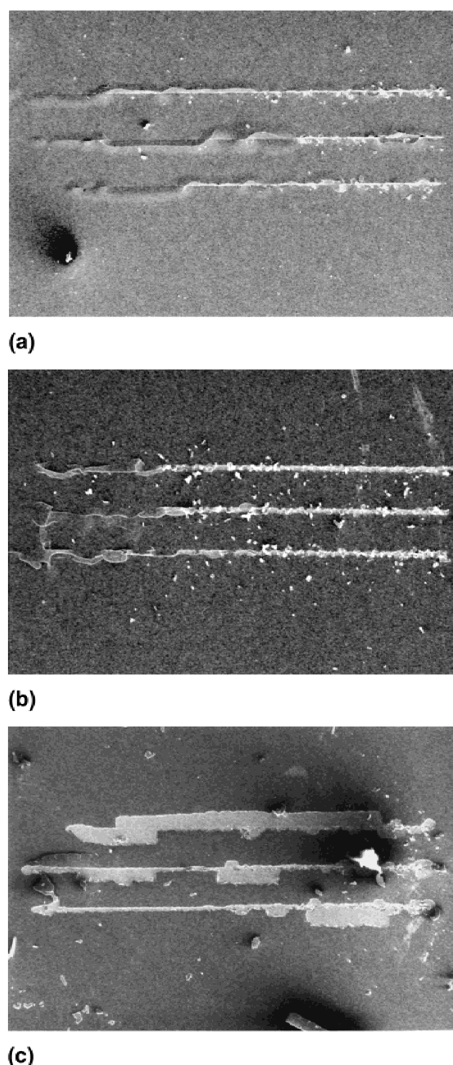

FIG. 17. SEM images (×149) of scratch tracks taken 2 months after scratching for the films with (a) 2.2 at.% N, (b) 20.2 at.% N, and (c) 40.2 at.% N.

12.8 GPa to reach the maximum value of 18.8 GPa. It is proposed that, in the course of incorporating more N, some N–B–N chains are generated at the interstitial sites, which cross-link the icosahedral clusters to enhance of the rigidity of the solid. At the same time, the *H*/*E* ratio increases steadily and is accompanied by a rise in the critical load. This shows that the wear resistance of the films is stronger with increasing N content. A simple calculation illustrates that the N content in the films is not high enough for both the B-rich phase and the graphitelike boron nitride phase to have the stoichiometric composition of the BN_4 and hexagonal BN structures, so that the theoretically strongest cross-linking effect occurring in the BN_4 structure has not been completely realized in the film samples. Further work is needed to determine what factors limit further incorporation of N and hinder successful formation of the ideal BN_4 structure. Furthermore, the films with low N contents are relatively ductile.

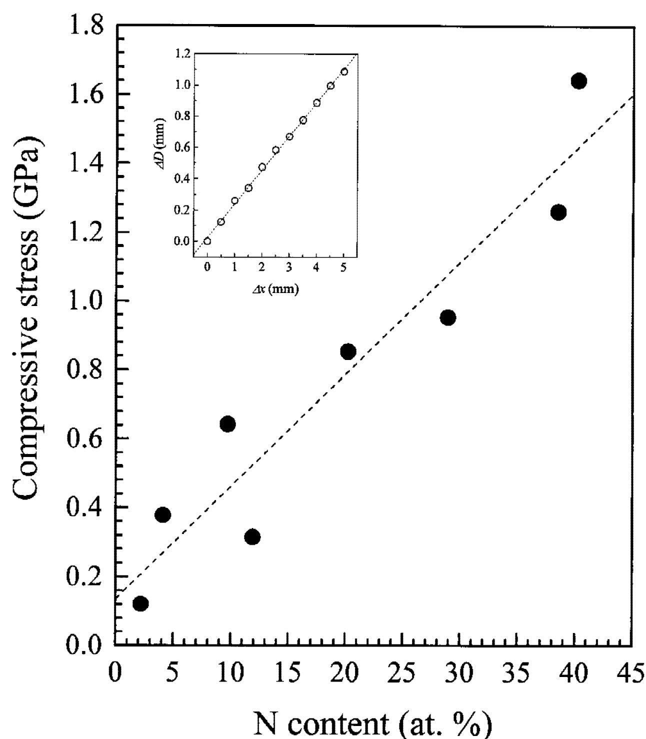

FIG. 18. Internal stress on the films with various N contents. Inset: Typical plot of deflection of the laser beam against displacement of the film sample.

For films with higher N contents (>20.2 at.%), the hardness drops continuously to the lowest value of 13 GPa, attributable to growth of the relatively soft graphitelike boron nitride phase. However, the elastic modulus also drops synchronically, so that the *H*/*E* ratio is almost unchanged. As a consequence, the critical load remains almost unchanged, implying that the wear resistance of the films is not prominently altered with the N content. In addition, the films become more brittle.

Two general trends are found for all the specimens. First, the friction coefficient μ of the film against diamond depends on the normal load L in the form $\mu = aL^y$, where a and y are numerical parameters. It is found that the values of a and y are not sensitive to the change in the N content. Second, compressive stress is found to exist in all the films, and it increases from about 0.12 to 1.7 GPa with the N content increasing in the range observed. Owing to the presence of stress, the peeling off of the film around the scratch track is accelerated. Meanwhile, the adhesion stability of the films can be reflected, at least qualitatively, by the speed of peeling off and the propagation of the scratch track.

ACKNOWLEDGMENTS

The work described in this paper was supported by grants from the Hong Kong Polytechnic University (Code Nos. G-V269, A-P106, and G-S850), and by a grant from

CAMBRIDGE JOURNALS
http://journals.cambridge.org Downloaded: 27 Aug 2013 IP address: 158.132.161.52

the Research Grants Council of the Hong Kong Special Administrative Region (Project No. HKP31/95P).

REFERENCES

1. O.A. Golikova, Phys. Status Solidi A **101,** 277 (1987).
2. R. Riedel, Adv. Mater. **6,** 549 (1994).
3. T. Lundström and Y.G. Andreev, Mater. Sci. Eng. A **209,** 16 (1996).
4. T.L. Aselage and R.G. Tissot, J. Am. Ceram. Soc. **75,** 2207 (1992).
5. H. Hubert, L.A.J. Garvie, B. Devouard, P.R. Buseck, W.T. Petuskey, and P.F. McMillan, Chem. Mater. **10,** 1530 (1998).
6. H. Saitoh, K. Yoshida, and W.A. Yarbrough, J. Mater. Res. **8,** 8 (1993).
7. X-A. Zhao, C.W. Ong, K.F. Chan, Y.M. Ng, Y.C. Tsang, C.L. Choy, and P.W. Chan, J. Vac. Sci. Technol. A. **15,** 2297 (1997).
8. D.A. Shirley, Phys. Rev. B **5,** 4709 (1972).
9. A. Witvrouw and F. Spaepen, in *Thin Films: Stresses and Mechanical Properties II,* edited by M.F. Doerner, W.C. Oliver, G.M. Pharr, and F.R. Brotzen (Mater. Res. Soc. Symp. Proc. **188,** Pittsburgh, PA, 1990), p. 147.
10. G.G. Stoney, Proc. R. Soc. London, Ser. A **8,** 172 (1909).
11. W.A. Brantley, J. Appl. Phys. **44,** 534 (1973).
12. C.W. Ong, K.P. Chik, and H.K. Wong, J. Appl. Phys. **74,** 6094 (1993).
13. T.A. Friedmann, K.F. McCarty, E.J. Klaus, J.C. Barbour, W.M. Clift, H.A. Johnsen, D.L. Medlin, and D.K. Ottesen, Thin Solid Films **237,** 48 (1994).
14. O.A. Golikova, M. Zhubanov, and D.N. Mirlin, Sov. Phys. Solid State **11,** 1341 (1969).
15. C.W. Ong, K.P. Chik, and H.K. Wong, J. Non-Cryst. Solids **114,** 783 (1989).
16. W. Dworschak, K. Jung, and H. Ehrhardt, Thin Solid Films **254,** 65 (1995).
17. P.B. Mirkarimi, K.F. McCarty, D.L. Medlin, W.G. Wolfer, T.A. Friedmann, E.J. Klaus, G.F. Cardinale, and D.G. Howitt, J. Mater. Res. **9,** 2925 (1994).
18. J.F. Moulder, W.F. Stickle, P.E. Sobol, and K.D. Bomben, *Handbook of X-ray Photoelectron Spectroscopy* (Perkin-Elmer Corporation, Eden Prairie, MN, 1992), p. 215.
19. B. Rother, C. Weissmantel, and G. Leonhardt, Phys. Status Solidi A **100,** 553 (1987).
20. M. Okamoto, Y. Utsumi, and Y. Osaka, Jpn. J. Appl. Phys. **29,** L1004 (1990).
21. M.O. Watanabe, S. Itoh, and K. Mizushima, Appl. Phys. Lett. **68,** 2962 (1996).
22. C. Doughty, S.M. Gorbatkin, T.Y. Tsui, G.M. Pharr, and D.L. Medlin, J. Vac. Sci. Technol., A **15,** 2623 (1997).
23. T.Y. Tsui, G.M. Pharr, W.C. Oliver, Y.W. Chung, E.C. Cutiongco, C.S. Bhatia, R.L. White, R.L. Rhoades, and S.M. Gorbatkin, in *Thin Films: Stresses and Mechanical Properties V,* edited by S.P. Baker, C.A. Ross, P.H. Townsend, C.A. Volkert, and P. Børgesen (Mater. Res. Soc. Symp. Proc. **356,** Pittsburgh, PA, 1995), p. 767.
24. K. Miyoshi, Surf. Coat. Technol. **36,** 487 (1988).

CAMBRIDGE JOURNALS
http://journals.cambridge.org Downloaded: 27 Aug 2013 IP address: 158.132.161.52